

6-25-2024

## Microencapsulation of *Cosmos caudatus* Kunth Extract using Sodium Alginate and In Vitro Antioxidant Activity Test

Safina Samara Nur Fadlila

*Chemistry Department, Faculty of Mathematics and Natural Sciences, Universitas Brawijaya, Malang 65145, Indonesia*

Oktavia Eka Puspita

*Department of Pharmacy, Faculty of Medicine, Universitas Brawijaya, Malang 65145, Indonesia*

Zubaidah Ningsih

*Chemistry Department, Faculty of Mathematics and Natural Sciences, Universitas Brawijaya, Malang 65145, Indonesia*

Anna Safitri

*Chemistry Department, Faculty of Mathematics and Natural Sciences, Universitas Brawijaya, Malang 65145, Indonesia, a.safitri@ub.ac.id*

Follow this and additional works at: <https://scholarhub.ui.ac.id/science>



Part of the [Medicinal-Pharmaceutical Chemistry Commons](#), [Natural Products Chemistry and Pharmacognosy Commons](#), [Other Pharmacy and Pharmaceutical Sciences Commons](#), and the [Pharmaceutics and Drug Design Commons](#)

---

### Recommended Citation

Fadlila, Safina Samara Nur; Puspita, Oktavia Eka; Ningsih, Zubaidah; and Safitri, Anna (2024)

"Microencapsulation of *Cosmos caudatus* Kunth Extract using Sodium Alginate and In Vitro Antioxidant Activity Test," *Makara Journal of Science*: Vol. 28: Iss. 2, Article 1.

DOI: 10.7454/mss.v28i2.2298

Available at: <https://scholarhub.ui.ac.id/science/vol28/iss2/1>

This Article is brought to you for free and open access by the Universitas Indonesia at UI Scholars Hub. It has been accepted for inclusion in Makara Journal of Science by an authorized editor of UI Scholars Hub.

## Microencapsulation of *Cosmos caudatus* Kunth Extract using Sodium Alginate and *In Vitro* Antioxidant Activity Test

Safina Samara Nur Fadlila<sup>1</sup>, Oktavia Eka Puspita<sup>2</sup>, Zubaidah Ningsih<sup>1</sup>, and Anna Safitri<sup>1\*</sup>

1. Chemistry Department, Faculty of Mathematics and Natural Sciences, Universitas Brawijaya, Malang 65145, Indonesia  
2. Department of Pharmacy, Faculty of Medicine, Universitas Brawijaya, Malang 65145, Indonesia

\*E-mail: a.safitri@ub.ac.id

Received November 8, 2023 | Accepted May 11, 2024

### Abstract

This study aims to encapsulate *Cosmos caudatus* K. leaf extract in sodium alginate crosslinked with calcium chloride (CaCl<sub>2</sub>) as coating materials through freeze-drying. Antioxidant assays were performed to evaluate the applicability of the microcapsules as antidiabetic medicines. Their characteristics, antioxidant activity, and encapsulation efficiency (EE) were also examined. Results indicated that the concentration of sodium alginate and pH influenced the manufacturing process of the microcapsules. The highest EE was obtained at pH 6 and alginate concentration of 2% (w/v). The IC<sub>50</sub> for the antioxidant activity of the microcapsules was 139.96 ± 1.094 µg/mL. Scanning electron microscopy confirmed the presence of irregular and spherical structures on the surface. Fourier transform infrared spectra showed new absorption bands at 1593.10 and 1427.59 cm<sup>-1</sup>, demarcating the existence of stretching vibrations of COO<sup>-</sup>. Absorption at 1024.14 cm<sup>-1</sup> demonstrated C–C and C–O bond stretching vibrations in the sodium alginate–CaCl<sub>2</sub> crosslinks. Fourier transform infrared spectrum analyses indicated that sodium alginate and CaCl<sub>2</sub> formed chemical bonds, enabling microencapsulation. This study discovered that microencapsulation is a highly prospective and adaptable strategy for enhancing the medicinal use of plant extract.

**Keywords:** alginate, antioxidant, *Cosmos caudatus* Kunth, microencapsulation, freeze-drying

### Introduction

*Cosmos caudatus* Kunth is a member of the *Asteraceae* family native to Central America and can be found in Indonesia and other Asian countries. The high concentrations of flavonoids and phenolics in *C. caudatus* K. contribute to its pharmacological effects. Among the studied substances, quercetin exhibits some of the best antioxidant and antiobesity properties, reducing oxidative stress on cells and lowering the risk of developing diabetes mellitus [1]. *C. caudatus* K. contains antidiabetic, antioxidant, antihypertensive, and antiinflammatory properties [2]. In vitro research demonstrated the antioxidant activity of the flavonoid components in *C. caudatus* K. leaf extracts. The identified flavonoids, including genistin, roxoxin B, and quercetin, possess a high antioxidant capacity and various medicinal properties. The antioxidant properties of *C. caudatus* K. have potential health benefits, including protection against oxidative stress and chronic diseases [3–5].

Owing to human lifestyle changes and increasing affluence, diabetes mellitus is currently on the rise. This disease can lead to significant morbidity and mortality rates due to vascular consequences. Another illness complication is

hypercholesterolemia, which is characterized by blood cholesterol levels exceeding the normal range of 240 mg/dL [6]. According to World Health Organization (WHO) data in 2014, the prevalence of diabetes was 8.5% among adults aged 18 years and older. Diabetes was a direct cause of 1.6 million mortalities in 2016, and increased blood glucose levels were a contributing factor to 2.2 million mortalities in 2021 [7].

The current treatment approach for diabetes mellitus focuses on maintaining normal blood glucose levels. However, synthetic medications often have adverse effects that seriously harm the patients' health during treatment. As an alternative form of treatment, the pharmacological potential of medicinal plants has been studied. According to the WHO, 75%–80% of the global population continuously depends on traditional medicine practices rooted in plants. This reliance is especially prominent in developing countries with abundant plant diversity, such as Indonesia. *Cosmos caudatus* K. is one of the medicinal plants with therapeutic potential [2].

Oral drug distribution is the most commonly used method due to high patient compliance, modification of dosage forms, and cost-effective manufacturing [8]. The limited

bioavailability of drugs is a major limitation associated with oral drug administration. This challenge arises from the physicochemical characteristics of medications, such as low water solubility and membrane permeability, which may hinder their absorption in the gastrointestinal tract. Chemical and biological stability can also complicate the absorption process and physiological barriers, such as pH, efflux transporters, metabolic enzymes, and potential local discomfort and nausea [9]. Quercetin, a polyphenolic flavonoid and a highly hydrophobic medication, is utilized as an antioxidant. It inhibits cell growth and prevents cancer development, offering effective treatment for breast, ovarian, colon, and lung cancers. Owing to its limited ability to dissolve in liquids and low absorption into the body, its effectiveness could be improved [10]. However, quercetin compounds have limited bioavailability due to their rapid degradation and decreased absorption, and their conjugated form or metabolites cannot fully realize the expected health benefits. Given that quercetin components can be found in *C. caudatus* K. leaf extract, modification is required to enhance their bioavailability through microencapsulation [11]. This technique shields the core substance from external influences, masks unpleasant tastes and odors, chemically and physically blends poorly miscible substances, controls the release of the core substance, and enhances stability [12].

Microencapsulation can shield and preserve the extract's active chemicals for a long time, preventing a decrease in their concentration when the extract enters the body's circulation [13]. Choosing a suitable drying method is essential for encapsulation. Freeze-drying is one of the most common techniques for drying [14]. The effectiveness of encapsulation and the stability of the produced microcapsules are both influenced by the choice of material for microencapsulation. Under ideal circumstances and predetermined times, the proper encapsulating material will release the core substance. Sodium alginate is an encapsulating substance employed in microencapsulation [15]. When reacting with monovalent metal ions, sodium alginate produces soluble salts; when reacting with divalent and multivalent cations, it produces gels or precipitates. Calcium-induced alginate polymerization depends on the formation of ionic crosslinks between  $\text{Ca}^{2+}$  cations and alginate anions. Ionic bonds bind each  $\text{Na}^+$  cation [16]. To date, only a few studies have focused on the effects of solvent pH, sodium alginate concentration, and stirring time during microencapsulation. Given that sodium alginate contains acid groups such as mannuronic and guluronic acids, it dissolves well in acidic liquids. In microencapsulation, choosing the proper solvent pH is essential because it can alter encapsulation efficiency (EE) [17]. The efficiency and yield of encapsulation are influenced by the concentration of calcium chloride ( $\text{CaCl}_2$ ) solution [18].

The success rate of microencapsulation is determined by the EE, which represents the percentage of the active substances, such as flavonoids, effectively protected by the microcapsules. A high EE indicates that the encapsulating material provides good protection [19]. A previous study microencapsulated ethanolic extract from *C. caudatus* K. leaves using spray drying under varying pH, chitosan concentrations as the encapsulating material, and stirring times [2]. However, the microencapsulation of ethanolic extract from *C. caudatus* K. leaves using sodium alginate as the encapsulating substance has never been investigated. The present study aimed to encapsulate the extract of *C. caudatus* K. leaves using sodium alginate crosslinked with  $\text{CaCl}_2$  as coating materials through freeze-drying. Moreover, the antioxidative properties of the encapsulated extract were determined. The effect of manufacturing parameters, such as pH and sodium alginate concentration, was also evaluated. The microcapsules' properties, EE, and antioxidant activity were examined.

## Methods

**Materials and instrumentations.** The materials in this study consisted of *C. caudatus* K. powdered leaves procured from the UPT (*Unit Pelaksana Teknis*) Laboratory Herbal *Materia Medica* in Batu, East Java, Indonesia. This research utilized the following chemicals from Merck: anhydrous  $\text{CaCl}_2$ , ethyl alcohol (99.7%), glacial acetic acid (a secondary pharmaceutical standard), aluminum chloride ( $\text{AlCl}_3$ ), 3,5-dinitrosalicylic acid (DNS) reagent ( $\geq 98\%$ , HPLC grade), 2,2-diphenyl-1-picrylhydrazyl (DPPH, reagent grade), Tween-80, sodium alginate (a pharmaceutical secondary standard), and soluble starch (derived from potatoes, ACS grade). The equipment consisted of a Shimadzu UV-Vis spectrophotometer, a Shimadzu Prestige 21 Fourier Transform Infrared (FTIR) spectrometer, and a Hitachi TM 3000 scanning electron microscope (SEM).

**Preparation of *C. caudatus* K. Ethanolic extract.** In brief, 250 g of *C. caudatus* K. leaf powder was macerated in 1000 mL of 96% ethanol for three 24-hour periods. The resulting extract was filtered to separate the filtrate from the residue using cotton and a hydraulic press. After the *C. caudatus* K. leaf extract was obtained, the filtrate was concentrated using a rotary evaporator at 50 °C and 120 rpm. For additional characterization procedures, the extract was kept in a freezer at 40 °C [2].

**Microencapsulation of *C. caudatus* K. Ethanolic Extract.** The crude *C. caudatus* K. extract (0.5 g) was diluted in 2 mL of 96% ethanol and then slowly added with 10 mL of 2% sodium alginate solution (w/v) in 2% acetic acid solution (v/v) with pH variations of 4, 5, 6, and 7. The mixture was stirred using a magnetic stirrer at 300 rpm. With the use of a syringe, the mixture was slowly dropwise added into a 40 mL solution of  $\text{CaCl}_2$

(0.1 M). The resulting solution was then further stirred for 30 min using a magnetic stirrer. The obtained alginate beads were washed with distilled water to eliminate any residual  $\text{CaCl}_2$  adhering to their surface and then freeze-dried for 6 h at  $-55^\circ\text{C}$  and  $-60$  mmHg air pressure, resulting in their transformation into a fine powder consisting of microcapsules. The same procedure was replicated under various conditions using sodium alginate concentrations of 1%, 1.5%, 2%, and 2.5% (w/v). The initial pH that resulted in the highest percentage of EE (%EE) was utilized in this experiment, which was also performed under different conditions. The microcapsules' optimal conditions were estimated by utilizing the maximum percentage of %EE [20].

**Determination of total flavonoid content.** The microcapsules and *C. caudatus* K. extract were precisely weighed at 0.05 g each and then dissolved in 5 mL of methanol. The solution was poured into a test tube, which was then heated for 45 min at  $40^\circ\text{C}$  and rotated in a centrifuge for 10 min. After being carefully placed in a test tube, the mixture was added with 0.6 mL of a 2%  $\text{AlCl}_3$  solution and thoroughly mixed. The solution was left to incubate at room temperature for 23 min. A UV-vis spectrophotometer was used to measure the absorbance at a wavelength of 420 nm. The experiment was conducted three times. The total flavonoid content for each sample was determined by utilizing the standard quercetin curve and expressed as milligram of quercetin equivalent per gram of the sample [2].

**EE.** The microencapsulation efficiency level indicates the degree to which the coating material effectively encapsulates and protects the extract [2]. Equation (1) was used to determine the EE:

$$\text{Encapsulation efficiency (\%)} = \frac{\text{Total flavonoid content in microcapsules}}{\text{Total flavonoid content in extracts}} \times 100\% \quad (1)$$

**Antioxidant activity test.** Sample solutions were prepared using different quantities: 40–1200  $\mu\text{g/mL}$  for *C. caudatus* K. extracts, 120–200  $\mu\text{g/mL}$  for the microcapsules, and 2–12  $\mu\text{g/mL}$  for ascorbic acid. A 50  $\mu\text{g/mL}$  DPPH solution in 2 mL volume was added to each sample solution. The solutions were then left to incubate at room temperature for 30 min and stored in a light-free environment. Their absorbance at a wavelength of 516 nm was measured using a UV-vis spectrophotometer. The experiments were performed at triplicate. The antioxidant activity percentage was determined using Equation (2):

$$\text{Antioxidant activity (\%)} = \frac{\text{Absorbance control} - \text{Absorbance sample}}{\text{Absorbance control}} \times 100\% \quad (2)$$

$\text{IC}_{50}$ , the concentration at which 50% of the antioxidant activity is inhibited, was calculated using a linear regression equation. The x-axis represents the sample concentration, and the y-axis represents the percentage of antioxidant activity. This method assists in the determination of the  $\text{IC}_{50}$  by analyzing the slope of the regression line that passes through the data points [5].

**Fourier Transform Infrared (FTIR) and Scanning Electron Microscopy (SEM) analyses.** Samples for FTIR spectroscopy were prepared by dehydrating and compressing them into KBr pellets. Measurements were performed using a Shimadzu-type IR Prestige-21 FTIR, and observations were conducted throughout the wavenumber range of  $4000\text{--}400\text{ cm}^{-1}$ , including the infrared area of the spectrum. In addition to FTIR analysis, SEM TM 3000 Hitachi was used to investigate the shape and morphology of the extract and microcapsules observed at magnifications ranging from 500x to 12,000x.

**Data analysis.** The test results for the antioxidant activity and microencapsulation of *C. caudatus* K. ethanol extract were examined using a variance normality test with Kolmogorov–Smirnov test. One-way ANOVA using the F-test was then carried out with a confidence level of 95% ( $p = 0.05$ ). Post-hoc Tukey HSD test was utilized to determine the statistically significant treatment differences. SPSS version 26 was the software applied for the statistical analysis of the data.

## Results and Discussion

**Effect of pH on EE.** The medium pH is a critical component of the microencapsulation process. Each encapsulating substance employed in the microencapsulation has different solubilities in acidic and alkaline environments [21]. The pH level impacts the carboxyl groups' charge in alginate molecules. When the pH of the emulsion exceeds the pKa, the carboxyl groups on alginate will ionize and become negatively charged, allowing them to form electrostatic connections with the cationic polymers and calcium ions. Nevertheless, the carboxyl groups of alginates are mostly negatively charged in a slightly acidic solution (pH of approximately 5). Thus, a neutral pH maximizes the interaction between alginate and encapsulating materials, such as cationic polymers and calcium ions, while preventing harmful effects on the living cells in an overly acidic or alkaline environment [16].

The microcapsule sample with pH 6 has the maximum EE of 82.4 as shown in Table 1. The optimal pH for alginate microcapsules is determined by the pKa range of sodium alginate, which ranges between 3.4 and 4.4. When the pH of the emulsion exceeds its pKa, the carboxylate groups present in sodium alginate become ionized and form electrostatic bonds with the cationic

**Table 1. Percentage of Encapsulation Efficiency (%EE) of the Microcapsules at Various pH Levels**

Sample*	Encapsulation efficiency (%EE)**
Microcapsule pH 4	44.9 <sup>b</sup>
Microcapsule pH 5	59.6 <sup>c</sup>
Microcapsule pH 6	82.3 <sup>d</sup>
Microcapsule pH 7	74.6 <sup>a</sup>

\*The microcapsules were prepared by stirring 2% (w/v) sodium alginates for 30 min; \*\*Different notations, as determined by One-Way ANOVA with a confidence level of  $\alpha = 5\%$ , signify notable variations among the conditions.

polymers and calcium ions [22]. At a mildly acidic pH (6) where alginate dissociates efficiently, the divalent ion  $\text{Ca}^{2+}$  derived from the cross-linking agent  $\text{CaCl}_2$  can replace the  $\text{Na}^+$  ions and form ionic bonds with the carboxylate ions in alginate. As a consequence, a large amount of bioactive chemicals are encapsulated, boosting the EE [20, 21]. This finding is similar to a previous study [20], which concluded that pH 6 yielded the best results for sodium alginate-coated microcapsules. This pH level facilitates the dissociation of sodium alginate, allowing calcium ions ( $\text{Ca}^{2+}$ ) from  $\text{CaCl}_2$  to replace sodium ions ( $\text{Na}^+$ ). Hence, the binding of different molecules is enhanced. In addition, the durability of small capsules is strengthened by forming chemical bonds between the repulsion of negatively charged alginate molecules and the attraction of positively charged calcium ions [23]. Calcium ions ( $\text{Ca}^{2+}$ ) enhance the cross-linking process, forming a stable matrix that contains a significant number of bioactive molecules. Enhancing the matrix strengthens the microcapsules and fortifies the gel, resulting in improved resistance to degradation and controlled drug release [24]. Meanwhile, a low EE is observed for the microcapsules generated at pH 4 and 5. The amount of protonated sodium alginate molecules increases when the pH is between 4 and 5. The protonated form of sodium alginate may interrupt the binding between  $\text{Ca}^{2+}$  ions and  $\text{COO}^-$  ions, weakening the cross-linking bonds and microcapsule matrices. A decrease in the binding strength of the microcapsule matrix leads to a reduction in its ability to retain the extract, resulting in a low EE [20].

**Effect of polymer concentration on EE.** The microcapsules' size and EE can vary based on the quantity of sodium alginate used in the microencapsulation. Given that the sodium alginate concentration is under 1%, the number of carboxyl groups is insufficient for gel formation, producing few spherical capsules. High concentrations of sodium alginate result in great viscosity, forming large droplets with a varied size distribution [16]. Microcapsules with varying sodium alginate concentrations (1%, 1.5%, 2%, and 2.5% w/v) in 1% acetic acid (w/v) at the optimal pH 6 were produced to determine the optimum sodium alginate concentration.

The concentration of  $\text{CaCl}_2$  as a cross-linking agent and the duration of stirring were held constant at 0.1 M and 30 min, respectively.

Table 2 shows the correlation between the concentration of sodium alginate and the percentage of EE. The microcapsule sample with a sodium alginate concentration of 2% (w/v) demonstrates the highest EE of 85.5%. Increasing the quantity of sodium alginate within the 1% to 2% concentration range has led to an increase in EE. When the sodium alginate concentration increases, a significant number of  $\text{COO}^-$  ions. The link between alginate and calcium ions strengthens as the synthesis of  $\text{COO}^-$  ions increases, forming a dense and cohesive network. As a consequence, the space within the microcapsule shrinks. This characteristic enables the microcapsule to accommodate a high concentration of active molecules, thereby increasing the EE [25]. When the concentration of sodium alginate is 2.5%, the EE decreases because of an imbalance between the quantities of  $\text{COO}^-$  and  $\text{Ca}^{2+}$  ions during the microencapsulation. A high concentration of sodium alginate produces a large amount of  $\text{COO}^-$  ions, but a constant concentration of  $\text{CaCl}_2$  usually generates a constant amount of  $\text{Ca}^{2+}$  ions. The unbalanced ion concentration causes few cross-linking bonds to be formed, thus decreasing the EE [26].

Previous research demonstrated similar results [27]. The ideal concentration of sodium alginate for microencapsulating gallic acid differed from the highest concentration utilized. Several studies also demonstrated that the EE could be reduced when a low concentration of sodium alginate is used, depending on the specific combination of experimental factors [28, 29]. This behavior can be attributed to the increased alginate concentration that causes the solution to become highly viscous, trapping a significant amount of the bioactive ingredients [30]. Nonspherical capsules are formed when

**Table 2. Percentage Encapsulation Efficiency (%EE) of Microcapsules Prepared with Various Concentrations of Sodium Alginate**

Sample*	Encapsulation Efficiency (%)**
Microcapsules with 1% (w/v) sodium alginate concentration	52.9 <sup>b</sup>
Microcapsules with 1.5% (w/v) sodium alginate concentration	67.9 <sup>c</sup>
Microcapsules with 2% (w/v) sodium alginate concentration	85.7 <sup>d</sup>
Microcapsules with 2.5% (w/v) sodium alginate concentration	36.2 <sup>a</sup>

\*The microcapsules were prepared by stirring 2% (w/v) sodium alginates for 30 min; \*\*Different notations, as determined by the One-Way ANOVA test with a confidence level of  $\alpha = 5\%$ , signify notable variations among the conditions.

the concentration of sodium alginate is less than 1%, most likely because of the insufficient number of carboxyl groups for the gelling process. As a consequence, inadequate cross-linking between the alginate molecules occurs, forming capsules with irregular shapes and sizes. By contrast, if the concentration of sodium alginate exceeds 5%, the viscosity of the water-based solution increases, resulting in large droplets with a broad range of sizes. This phenomenon occurs due to the solution's increased ability to form a gel, creating significant and consistent capsules at high concentrations of sodium alginate. The high viscosity also helps stabilize the capsules, increasing their resistance to breaking down and guaranteeing a uniform release of the substances inside the body [22].

**Antioxidant activity.** The antioxidant activity was assayed using the DPPH reagent. Radical DPPH is an organic substance that consists of unstable nitrogen, resulting in a dark purple solution color. The antioxidant chemicals in the sample solution will absorb the free radicals of the DPPH solution by releasing hydrogen (H) atoms, creating a new reduced molecule called DPPH-H. As a consequence, a colorless solution is produced [31]. Table 3 shows the antioxidant activity test results. Ascorbic acid was utilized as the positive control. The uncapsulated *C. caudatus* K. extract was also examined and compared with the microcapsules.

Among the substances, ascorbic acid exhibits the highest levels of antioxidant activity with an  $IC_{50}$  of  $2.6 \pm 0.021$   $\mu\text{g/mL}$ . However, the microcapsules exhibit a lower antioxidant activity ( $IC_{50}$  of  $139.96 \pm 1.094$   $\mu\text{g/mL}$ ) than the uncapsulated extract ( $IC_{50}$  of  $75.56 \pm 0.091$   $\mu\text{g/mL}$ ), which is in line with the expected properties of antioxidants. Ascorbic acid, also known as vitamin C, is a strong antioxidant and neutralizer of free radicals, which explains its high antioxidant activity. Despite having lower antioxidant activity than the extract, the microcapsules are still categorized as active antioxidants ( $100 < IC_{50} < 150$   $\mu\text{g/mL}$ ), indicating that they retain antioxidant capability to some extent. The *C. caudatus* K. microcapsules being categorized as active antioxidants and the extracts being classified as very active antioxidants suggests a difference in the EE in preserving the core material's antioxidant properties [32]. The decreased antioxidant activity of the microcapsules is due to several factors. The bioactive chemicals enclosed in

the microcapsules may not be fully released, leading to a decreased antioxidant activity. The main objective of microencapsulation is to safeguard and regulate the release of active chemicals, not to enhance their biological activity. The EE and quality of the microcapsules affect their ability to maintain the core material until they reach the target site, which can significantly impact their antioxidant activity [33]. Furthermore, the higher antioxidant activity of the crude extract compared with that of the microcapsules is due to the reduction in flavonoid compounds after drying. As an essential stage in the microencapsulation of flavonoid compounds, drying can result in the loss of these compounds. In this process, the flavonoid compounds might degrade or volatilize, resulting in a decrease in their concentration within the microcapsules. The microcapsules' antioxidant activity may also be reduced due to the decrease in flavonoid compounds [34]. This observation is consistent with a previous report that demonstrated similar findings. They discovered that the antioxidant activity of *R. tuberosa* L. and *C. caudatus* K. microcapsules was lower than that of their respective extracts and ascorbic acid. Nevertheless, the microcapsules in the current work exhibit a reduced antioxidant activity compared with the extract and ascorbic acid. The  $IC_{50}$  is  $123.97 \pm 9.33$   $\mu\text{g/mL}$  for the microcapsules,  $16.42 \pm 2.12$   $\mu\text{g/mL}$  for the extract, and  $1.28 \pm 0.23$   $\mu\text{g/mL}$  for ascorbic acid [5].

The strategy to enhance antioxidant activity after microencapsulation is demonstrated by increasing the concentration of wall materials. Increased concentrations of wall materials improve the retention of core components within microcapsules, potentially resulting in a heightened antioxidant activity. This concentration signifies the enhanced preservation of phenolic chemicals essential for retaining antioxidant capabilities. In addition, increased quantities of wall material contribute to the stability of microcapsules, which is crucial for retaining encapsulated antioxidants. Furthermore, the flexibility and molecular size of wall materials affect the movement of volatile and delicate substances on the surface of the microcapsule, which in turn influence the speed at which they are released and their antioxidant properties. Controlling the drying process and storage conditions can prevent the degradation of the encapsulated antioxidants, ensuring their regulated release. Incorporating release-enhancing agents can also improve the release rate of the encapsulated antioxidants, and optimizing the size and shape of the microcapsules can influence their stability and release properties [34, 35].

**FTIR and SEM analysis.** The prepared *C. caudatus* K. ethanol extract and microcapsules were analyzed using a FTIR spectrophotometer to specify their specific functional groups. The FTIR spectra are depicted in Figures 1(a) and 1(b), and the functional groups identified through absorption are detailed in Table 4.

**Table 3. Antioxidant Activity Test Results**

Sample	$IC_{50}^*$
Microcapsules prepared at optimum condition	$139.96 \pm 1.094^b$
Ethanol extract of <i>C. caudatus</i> K.	$75.56 \pm 0.091^c$
Ascorbic acid	$2.6 \pm 0.021^a$

\*Different notations, as determined by the One-Way ANOVA test with a confidence level of  $\alpha = 5\%$ , signify notable variations among the conditions.

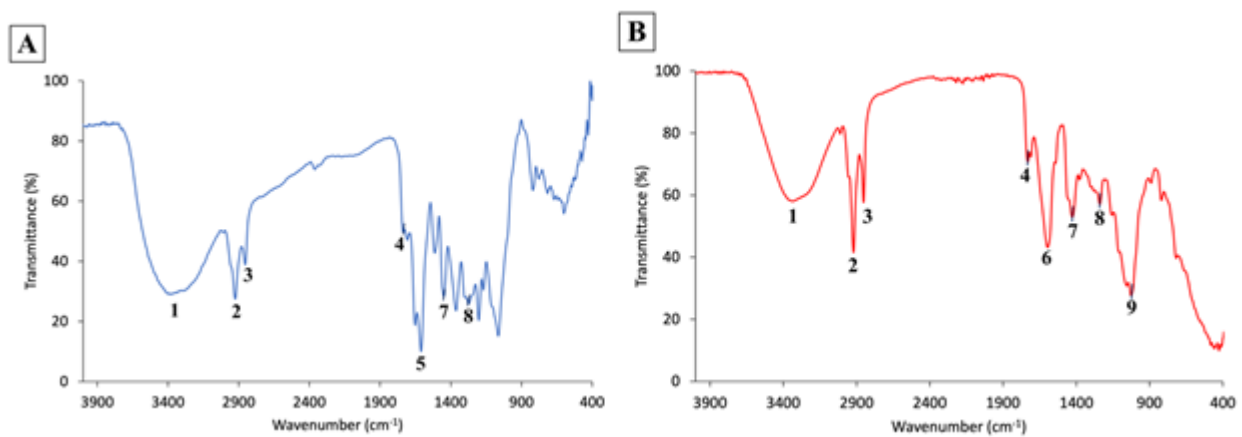


**Figure 1.** FTIR Spectra of the (a) *C. caudatus* K. extract. (b) *C. caudatus* K. Extract Microcapsules Prepared Under Solution pH 6, Stirring for 30 min, and 2% (w/v) Sodium Alginate

**Table 4.** Assignments of the Functional Group Spectra

Peak Number	<i>C. caudatus</i> K. extracts [33, 36–38]	Microcapsules of <i>C. caudatus</i> K. extracts [33, 36–38]
1	3386.21 cm <sup>-1</sup> for O–H alcohol	3331.03 cm <sup>-1</sup> for O–H alcohol
2	2924.24 cm <sup>-1</sup> for C–H aliphatic	2917.24 cm <sup>-1</sup> for C–H aliphatic
3	2848.28 cm <sup>-1</sup> for C–H aliphatic	2851.72 cm <sup>-1</sup> for C–H aliphatic
4	1741.38 cm <sup>-1</sup> for C=O ketones	1727.59 cm <sup>-1</sup> for C=O ketones
5	1610.34 cm <sup>-1</sup> for C=O ketones	
6		1593.10 cm <sup>-1</sup> for COO <sup>-</sup> asymmetric
7	1444.83 cm <sup>-1</sup> for C=C aliphatic rings	1427.59 cm <sup>-1</sup> for COO <sup>-</sup> symmetric
8	1272.41 cm <sup>-1</sup> for C–O–C aromatic ether	1241.38 cm <sup>-1</sup> for C–O–C aromatic ether
9		1024.14 cm <sup>-1</sup> for C–O–C aliphatic ether

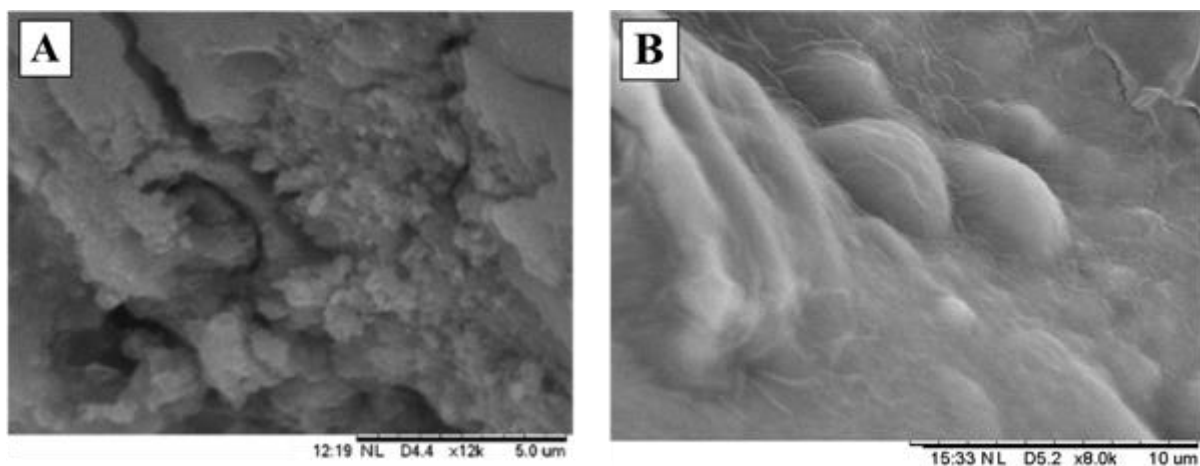


**Figure 2.** SEM Images of the (a) *C. caudatus* K. extract. (b) Microcapsules of *C. caudatus* K. Extract Prepared Under pH 6, 30 min Stirring Time, and 2% (w/v) Sodium Alginate

FTIR analysis showed the presence of functional groups in the extracts and microcapsules of *C. caudatus* K. Figure 1 displays the FTIR spectra, and Table 4 lists the assignments of the functional groups responsible for ab-

sorption. Figure 3(a) indicates that the extract of *C. caudatus* K. exhibits the stretching vibrations of the hydroxyl (O–H) group at a wavelength of 3386 cm<sup>-1</sup>. This finding is consistent with the general range for O–H stretching vibrations, which typically occur in the 3200–3600 cm<sup>-1</sup>

region. The separated peaks corresponding to the stretching of aliphatic C–H bonds are observed at 2294 and 2848  $\text{cm}^{-1}$ . The observed vibrations are consistent with the expected range for C–H stretching vibrations, which typically appear in the area of 2800–3300  $\text{cm}^{-1}$  [36]. The absorption peaks at 1741.38 and 1610.34  $\text{cm}^{-1}$  are caused by the stretching of C=O bonds. The C=O stretching vibrations indicate the existence of carbonyl groups, which are frequently found in carboxylic acids, aldehydes, and ketones. The peaks observed at 1444.83 and 1272.41  $\text{cm}^{-1}$  are attributed to the stretching vibrations of aromatic C=C bonds and aromatic ether C–O–C bonds, respectively. The observed frequencies are within the predicted ranges for aromatic C=C stretching vibrations (1400–1500  $\text{cm}^{-1}$ ) and aromatic ether C–O–C stretching vibrations (1200–1300  $\text{cm}^{-1}$ ). The presence of aromatic rings and aromatic ether groups in compounds is indicated by the stretching vibrations of C=C and C–O–C bonds. These vibrations are characteristic of the compounds containing phenolic groups or other aromatic structures [37]. The observed absorptions indicate the presence of flavonoid compounds in *C. caudatus* K [38]. A previous study showed that the wavenumber around 1617.32  $\text{cm}^{-1}$  indicated the specific absorption of *C. caudatus* K. extract [5]. This finding is consistent with the current assignment of FTIR spectra for *C. caudatus* K. extracts, where the peak at 1610.34  $\text{cm}^{-1}$  is attributed to C=O ketone functional groups. This spectral characteristic is crucial for identifying and analyzing the bioactive compounds in *C. caudatus* K. extracts because it serves a unique fingerprint for this plant species.

The FTIR spectra of the microcapsules demonstrate a shift in the stretching vibrations of the C=O carbonyl, O–H alcohol, C–H aliphatic, and C–O–C aromatic ether at peaks 1, 2, 3, 4, and 7, respectively [5]. Peak number 5 appears in Figure 1(a) but not in Figure 1(b). The peak number 6 in Figure 1(b) is located at 1593.10 and 1427.59  $\text{cm}^{-1}$ , representing a new absorption peak. This peak is attributed to the asymmetric and symmetric stretching vibrations of the COO– groups. These absorptions suggest the formation of a chemical bond (ionic bonding) between sodium alginate and  $\text{CaCl}_2$  as a cross-linking agent. Moreover, the appearance of a new absorption peak at 1024.14  $\text{cm}^{-1}$  indicates the presence of C–O–C aliphatic ether stretching vibrations, which can also be attributed to the cross-linking between sodium alginate and  $\text{CaCl}_2$  [39]. The FTIR spectra of the extracts and microcapsules of *C. caudatus* K. exhibit similarities, indicating that the microcapsules contain the bioactive chemicals isolated from *C. caudatus* K. These observed similarities suggest that the encapsulating technique is successful, as the microcapsules maintain the chemical properties of the original extracts. The differences in spectra between the microcapsules and extracts are primarily due to the encapsulation process, which adds new chemical interactions and structures within the microcapsules [40]. The above results are similar to the

analysis of microbead alginate in previous research [41], where the FTIR spectra showed specific peaks that correlated with the vibrational modes of the alginate structure. For example, the spectra of alginate-based polymers often show the presence of hydrogen-bonded OH groups, indicating that these materials can retain water. The C–H stretching vibrations are specific to the aliphatic chains in the alginate structure, and the C–O vibrations indicate the presence of carboxyl groups. These carboxyl groups are important for the cross-linking and the production of the 3D network structure of alginate.

SEM characterization of the obtained microcapsules revealed differences in surface morphology between the extracts and microcapsules as displayed in Figures 2(a) and 2(b), respectively. The microcapsules show an irregular morphology as identified by the presence of a few spherical shapes and a uniform pattern of wrinkled surfaces. This morphological characteristic is similar to the from a previous study, which indicated that freeze-dried materials generally lack a specific morphology [42]. SEM examination showed that the irregular morphology and wrinkled surfaces of the microcapsules may be directly attributable to the encapsulation process. The utilization of encapsulation techniques, such as freeze-drying, might result in the creation of microcapsules with irregular shapes and sizes due to the heterogeneity of the process. This procedure involves the rapid freezing of the solution containing the bioactive chemicals and the polymer, followed by a slow elimination of water, which may create ice crystals. These ice crystals may generate holes and contribute to the irregular morphology of the freeze-dried substance, including the microcapsules [43]. The morphology of the microcapsules, characterized by their spherical shape and wrinkled surfaces, significantly influences their effectiveness as drug delivery systems. Their spherical shape suggests that the extract's active ingredients are properly coated, which is essential for encapsulation. This coating protects the active ingredients from degradation and facilitates a controlled release of the therapeutic candidate through diffusion, dissolution, osmosis, and erosion. These mechanisms are influenced by the physical characteristics of the microcapsules, including their dimensions, configuration, and surface morphology. By contrast, the nonspherical form of the microcapsules indicates the existence of empty spaces, which may result in a fast release of the encapsulated drug. This feature may not be favorable in certain therapeutic situations because it can result in an unexpected peak in drug levels, which could lead to toxicity or reduce the overall efficacy of the treatment [44, 45].

## Conclusion

The microencapsulation of *C. caudatus* K. extracts using a freeze-drying technique with sodium alginate and

calcium chloride as wall materials was successfully investigated, revealing its potential implementation in bioactive compounds from plant nutraceuticals. The optimum conditions for this process were pH 6 and 2% (w/v) sodium alginate concentration. The microcapsules demonstrated potential as natural antioxidants, indicated by their  $IC_{50}$  of  $139.96 \pm 1.094$   $\mu\text{g/mL}$ . FTIR analysis confirmed the formation of a cross-linking between sodium alginates and calcium chloride, which is crucial for the stability and functionality of the microcapsules. Morphological analysis using SEM revealed that the microcapsules had an irregular morphology with a uniform distribution of wrinkled surfaces and a few spherical shapes. This irregular morphology suggested that the microencapsulation process was successful in coating the bioactive compounds from the extract, even though it was not optimal for the consistent delivery of active compounds. The results indicated that *C. caudatus* K. extract microencapsulation provides a novel way to exploit bioactive components from plant nutraceuticals, with potential applications in food and medicine. This work advanced our understanding of microencapsulation techniques but opened up new avenues for the development of bioactive pharmaceuticals and nutraceuticals. The prospects for this research are vast, with potential applications in enhancing the delivery of bioactive compounds, improving the stability of pharmaceuticals, and exploring new therapeutic strategies.

## Acknowledgements

This research was supported by the HPU Grant, Universitas Brawijaya, Indonesia, year of 2023 (Grant Number 612.56/UN10.C20/2023).

## References

- [1] Aghababaei, F., Hadidi, M. 2023. Recent advances in potential health benefits of quercetin. *Pharmaceuticals*. 16(7): 1020, <https://doi.org/10.3390/ph16071020>.
- [2] Safitri, A., Roosdiana, A., Hitdatania, E., Damayanti, S.A. 2021. in vitro alpha-amylase inhibitory activity of microencapsulated *Cosmos caudatus* kunth extracts. *Indones. J. Chem.* 22(1): 212, <https://doi.org/10.22146/ijc.68844>.
- [3] Latiff, N.A., Ong, P.Y., Abd Rashid, S.N.A., Abdullah, L.C., Amin, N.A.M., Fauzi, N.A.M. 2021. Enhancing recovery of bioactive compounds from *Cosmos caudatus* leaves via ultrasonic extraction. *Scientific Reports*, 11: 17297, <https://doi.org/10.1038/s41598-021-96623-x>.
- [4] Rafi, M., Hayati, F., Umar, A.H., Septaningsih, D.A., Rachmatiah, T. 2023. LC-HRMS-based metabolomics to evaluate the phytochemical profile and antioxidant capacity of *Cosmos caudatus* with different extraction methods and solvents. *Arab. J. Chem.* 16(9): 105065, <https://doi.org/10.1016/j.arabjc.2023.105065>.
- [5] Annisa, C., Prasetyawan, S., Safitri, A. 2022. Co-microencapsulation of *Ruellia tuberosa* L. and *Cosmos caudatus* K. extracts for pharmaceutical applications. *Makara J. Sci.* 26(2): 96–106, <https://doi.org/10.7454/mss.v26i2.1334>.
- [6] Fan, W. 2017. Epidemiology in diabetes mellitus and cardiovascular disease. *Cardiovasc. Endocrin.* 6(1): 8–16, <https://doi.org/10.1097/XCE.0000000000000116>.
- [7] Zimmet, P., Alberti, K.G., Magliano, D.J., Bennett, P.H. 2016. Diabetes mellitus statistics on prevalence and mortality: facts and fallacies. *Nat. Rev. Endocrinol.* 12: 616–622, <https://doi.org/10.1038/nrendo.2016.105>.
- [8] Ahadian, S., Finbloom, J.A., Mofidfar, M., Diltemiz, S.E., Nasrollahi, F., Davoodi, E., et al. 2020. Micro and nanoscale technologies in oral drug delivery. *Adv. Drug Deliver. Rev.* 157: 37–62, <https://doi.org/10.1016/j.addr.2020.07.012>.
- [9] Alqahtani, M.S., Kazi, M., Alsenaidy, M.A., Ahmad, M.Z. 2021. Advances in oral drug delivery. *Front. Pharmacol.* 12: 618411, <https://doi.org/10.3389/fphar.2021.618411>.
- [10] Bhalani, D.V., Nutan, B., Kumar, A., Singh Chandel, A.K. 2022. Bioavailability enhancement techniques for poorly aqueous soluble drugs and therapeutics. *Biomedicines*. 10(9): 2055, <https://doi.org/10.3390/biomedicines10092055>.
- [11] Chen, L., Gnanaraj, C., Arulselvan, P., El-Seedi, H., Teng, H. 2019. A review on advanced microencapsulation technology to enhance bioavailability of phenolic compounds: Based on its activity in the treatment of type 2 diabetes. *Trends Food Sci. Tech.* 85: 149–162, <https://doi.org/10.1016/j.tifs.2018.11.026>.
- [12] Calderón-Oliver, M., Ponce-Alquicira, E. 2022. The role of microencapsulation in food application. *Molecules*. 27(5): 1499, <https://doi.org/10.3390/molecules27051499>.
- [13] Mutmainah, M., Martono, Y., Puspitaningrum, I., Kusmita, L. 2021. Leaf extract microencapsulation of stevia rebaudiana bert using inulin-chitosan as anti-diabetes diet. *J. Trop. Pharm. Chem.* 5(3): 203–208, <https://doi.org/10.25026/jtpc.v5i3.270>.
- [14] Pudziuvelyte, L., Marksa, M., Sosnowska, K., Winnicka, K., Morkuniene, R., & Bernatoniene, J. (2020). Freeze-Drying Technique for Microencapsulation of Elsholtzia ciliata Ethanolic Extract Using Different Coating Materials. *Molecules*, 25(9), 2237. <https://doi.org/10.3390/molecules25092237>.
- [15] Mehta, N., Kumar, P., Verma, A. K., Umaraw, P., Kumar, Y., Malav, O. P., ... Lorenzo, J. M. (2022). Microencapsulation as a Noble Technique for the Application of Bioactive Compounds in the Food Industry: A Comprehensive Review. *Applied Sciences*, 12(3), 1424. <https://doi.org/10.3390/app12031424>.

- [16] Kłosowska, A., Wawrzyniczak, A., Feliczak-Guzik, A. 2023. Microencapsulation as a route for obtaining encapsulated flavors and fragrances. *Cosmetics*. 10(1): 26, <https://doi.org/10.3390/cosmetics10010026>.
- [17] Frent, O., Vicas, L., Duteanu, N., Morgovan, C., Jurca, T., Pallag, A., *et al.* 2022. Sodium alginate—natural microencapsulation material of polymeric microparticles. *Int. J. Mol. Sci.* 23(20): 12108, <https://doi.org/10.3390/ijms232012108>.
- [18] Łętocha, A., Miastkowska, M., Sikora, E. 2022. Preparation and characteristics of alginate microparticles for food, pharmaceutical and cosmetic applications. *Polymers*. 14(18): 3834, <https://doi.org/10.3390/polym14183834>.
- [19] Perkasa, D.P., Erizal, E., Purwanti, T., Tontowi, A.E. 2018. Characterization of semi-interpenetrated network alginate/gelatin wound dressing crosslinked at sol phase. *Indones. J. Chem.* 18(2): 367, <https://doi.org/10.22146/ijc.25710>.
- [20] Cáceres, L.M., Velasco, G.A., Dagnino, E.P., Chamorro, E.R. 2020. Microencapsulation of grapefruit oil with sodium alginate by gelation and ionic extrusion: optimization and modeling of crosslinking and study of controlled release kinetics. *Revista Tecnología y Ciencia*, 39: 41–61, <https://doi.org/10.33414/rtyc.39.41-61.2020>.
- [21] Azarpazhooh, E., Sharayei, P., Rui, X., Gharibi-Tehrani, M., Ramaswamy, H.S. 2022. Optimization of wall material of freeze-dried high-bioactive microcapsules with yellow onion rejects using simplex centroid mixture design approach based on whey protein isolate, pectin, and sodium caseinate as incorporated variables. *Molecules*. 27(23): 8509, <https://doi.org/10.3390/molecules27238509>.
- [22] Pertiwi, A.K., Annisa, C., Ningsih, Z., Safitri, A. 2023. Microencapsulation of *Ruellia tuberosa* L. extracts using alginate: preparation, biological activities, and release. *Indones. J. Chem.* 23(2): 321, <https://doi.org/10.22146/ijc.76821>.
- [23] Ramdhan, T., Ching, S.H., Prakash, S., Bhandari, B. 2019. Time dependent gelling properties of cuboid alginate gels made by external gelation method: Effects of alginate-CaCl<sub>2</sub> solution ratios and pH. *Food Hydrocolloid*. 90: 232–240, <https://doi.org/10.1016/j.foodhyd.2018.12.022>.
- [24] Łętocha, A., Miastkowska, M., Sikora, E. 2022. Preparation and characteristics of alginate microparticles for food, pharmaceutical and cosmetic applications. *Polymers*. 14(18): 3834, <https://doi.org/10.3390/polym14183834>.
- [25] Hartini, N., Ponrasu, T., Wu, J.-J., Sriariyanun, M., Cheng, Y.-S. 2021. Microencapsulation of curcumin in crosslinked jelly fig pectin using vacuum spray drying technique for effective drug delivery. *Polymers*. 13(16): 2583, <https://doi.org/10.3390/polym13162583>.
- [26] Essifi, K., Brahmi, M., Berraaouan, D., Ed-Daoui, A., El Bachiri, A., Fauconnier, M.-L., Tahani, A. 2021. Influence of sodium alginate concentration on microcapsules properties foreseeing the protection and controlled release of bioactive substances. *J. Chem.* 2021(1): 5531479, <https://doi.org/10.1155/2021/5531479>.
- [27] Fadhilah, S., Mohd Azam, N.A.N., Mat Amin, K.A. 2019. Sodium alginate film: The effect of crosslinker on physical and mechanical properties. *IOP Conf. Ser.-Mat. Sci.* 509: 012063, <https://doi.org/10.1088/1757-899X/509/1/012063>.
- [28] Essifi, K., Lakrat, M., Berraaouan, D., Fauconnier, M.-L., El Bachiri, A., Tahani, A. 2021. Optimization of gallic acid encapsulation in calcium alginate microbeads using box-behnken experimental design. *Polym. Bull.* 78: 5789–5814, <https://doi.org/10.1007/s00289-020-03397-9>.
- [29] Szekalska, M., Sosnowska, K., Czajkowska-Kośnik, A., Winnicka, K. 2018. Calcium chloride modified alginate microparticles formulated by the spray drying process: A strategy to prolong the release of freely soluble drugs. *Materials*. 11(9): 1522, <https://doi.org/10.3390/ma11091522>.
- [30] Huang, J., Bai, F., Wu, Y., Ye, Q., Liang, D., Shi, C., *et al.* 2019. Development and evaluation of lutein loaded alginate microspheres with improved stability and antioxidant. *J. Sci. Food Agr.* 99(11): 5195–5201, <https://doi.org/10.1002/jsfa.9766>.
- [31] Machado, A.R., Silva, P.M.P., Vicente, A.A., Souza-Soares, L.A., Pinheiro, A.C., Cerqueira, M.A. 2022. Alginate particles for encapsulation of phenolic extract from *Spirulina* sp. LEB-18: Physicochemical characterization and assessment of in vitro gastrointestinal behavior. *Polymers*. 14(21): 4759, <https://doi.org/10.3390/polym14214759>.
- [32] Baliyan, S., Mukherjee, R., Priyadarshini, A., Vibhuti, A., Gupta, A., Pandey, R.P., *et al.* 2022. Determination of antioxidants by DPPH radical scavenging activity and quantitative phytochemical analysis of *Ficus religiosa*. *Molecules*. 27(4): 1326, <https://doi.org/10.3390/molecules27041326>.
- [33] Safitri, A., Roosdiana, A., Kurnianingsih, N., Fatchiyah, F., Mayasari, E., Rachmawati, R. 2022. Microencapsulation of *Ruellia tuberosa* L. aqueous root extracts using chitosan-sodium tripolyphosphate and their in vitro biological activities. *Scientifica*. 2022(1): 9522463, <https://doi.org/10.1155/2022/9522463>.
- [34] Ferreira, L.M.D.M.C., Pereira, R.R., Carvalho-Guimarães, F.B.D., Remígio, M.S.D.N., Barbosa, W.L.R., Ribeiro-Costa, R.M., *et al.* 2022. Microencapsulation by spray drying and antioxidant activity of phenolic compounds from tucuma coproduct (*Astrocaryum vulgare* Mart.) almonds. *Polymers*. 14(14): 2905, <https://doi.org/10.3390/polym14142905>.

- [35] Sharayei, P., Azarpazhooh, E., Ramaswamy, H.S. 2020. Effect of microencapsulation on antioxidant and antifungal properties of aqueous extract of pomegranate peel. *J. Food Sci. Technol.* 57(2): 723–733, <https://doi.org/10.1007/s13197-019-04105-w>.
- [36] Pertiwi, A.K., Annisa, C., Ningsih, Z., Safitri, A. 2023. Microencapsulation of *Ruellia tuberosa* L. extracts using alginate: preparation, biological activities, and release. *Indones. J. Chem.* 23(2): 321, <https://doi.org/10.22146/ijc.76821>.
- [37] Nandiyanto, A.B.D., Oktiani, R., Ragadhita, R. 2019. How to read and interpret FTIR spectroscopy of organic material. *Indone. J. Sci. Technol.* 4(1): 97, <https://doi.org/10.17509/ijost.v4i1.15806>.
- [38] Latiff, N., Ong, P.Y., Abdullah, L.C., Rashid, S.N.A.A., Fauzi, N.A.M., Amin, N.A.M. 2020. Ultrasonic-Assisted Extraction (UAE) for enhanced recovery of bioactive phenolic compounds From *Cosmos caudatus* leaves. *Antioxidants.* 9, <https://doi.org/10.21203/rs.3.rs-143469/v1>.
- [39] Bialik-Wąs, K., Króllicka, E., Malina, D. 2021. Impact of the type of crosslinking agents on the properties of modified sodium alginate/poly(vinyl alcohol) hydrogels. *Molecules.* 26(8): 2381, <https://doi.org/10.3390/molecules26082381>.
- [40] Nwabor, O.F., Singh, S., Marlina, D., Voravuthikunchai, S.P. 2020. Chemical characterization, release, and bioactivity of *Eucalyptus camaldulensis* polyphenols from freeze-dried sodium alginate and sodium carboxymethyl cellulose matrix. *Food Qual. Saf.* 4(4): 203–212, <https://doi.org/10.1093/fqsafe/fyaa016>.
- [41] Feyissa, Z., Edossa, G.D., Gupta, N.K., Negera, D. 2023. Development of double crosslinked sodium alginate/chitosan based hydrogels for controlled release of metronidazole and its antibacterial activity. *Heliyon.* 9(9): e20144, <https://doi.org/10.1016/j.heliyon.2023.e20144>.
- [42] Moayyedi, M., Eskandari, M.H., Rad, A.H.E., Ziaee, E., Khodaparast, M.H.H., Golmakani, M.-T. 2018. Effect of drying methods (electrospraying, freeze drying and spray drying) on survival and viability of microencapsulated *Lactobacillus rhamnosus* ATCC 7469. *J. Funct. Food.* 40: 391–399, <https://doi.org/10.1016/j.jff.2017.11.016>.
- [43] Makouie, S., Alizadeh, M., Maleki, O., Khosrowshahi, A. 2020. Optimization of Wall Components for Encapsulation of Nigella Sativa Seed Oil by Freeze-Drying. *Indones. Food Sci. Tech. J.* 3(1): 1–9, <https://doi.org/10.22437/ifstj.v3i1.7857>.
- [44] Lengyel, M., Kállai-Szabó, N., Antal, V., Laki, A. J., Antal, I. 2019. Microparticles, microspheres, and microcapsules for advanced drug delivery. *Sci. Pharm.* 87(3): 20, <https://doi.org/10.3390/scipharm87030020>.
- [45] Julaeha, E., Puspita, W.R., Permadi, N., Harja, A., Nurjanah, S., Wahyudi, T., et al. 2024. Optimization of *Citrus aurantifolia* peel extract encapsulation in alginate-gelatin hydrogel microbeads for antibacterial wound dressing applications. *Carbohydrate polymer technologies and applications. Carbohydr. Polym. Technol. Appl.* 7: 100406, <https://doi.org/10.1016/j.carpa.2023.100406>.